Colloid Polym Sci 274:723–731 (1996)

ORIGINAL CONTRIBUTION

Orientation of polybutadiene chains in a thermoplastic elastomer

V. Abetz
A. Dardin
R. Stadler
J. Hellmann
E.T. Samulski
H.-W. Spiess

Received: 18 December 1995
Accepted: 21 February 1996

Dr. V. Abetz (✉) · A. Dardin · R. Stadler
J. Hellmann
Institut für Organische Chemie
Johannes Gutenberg-Universität Mainz
J.J. Becher Weg 18-20
55099 Mainz, FRG

H.-W. Spiess
Max-Planck-Institut für Polymerforschung
Ackermannweg 10
55021 Mainz, FRG

E.T. Samulski
University of North Carolina at Chapel Hill
Chemistry Department
Chapel Hill, North Carolina 27599-3290
USA

Abstract The orientation of polybutadiene chains in thermoplastic elastomers based on hydrogen bonding complexes is investigated under uniaxial deformation by two-dimensional small-angle neutron scattering (SANS), deuteron magnetic resonance spectroscopy (^{2}H-NMR), optical birefringence and infrared dichroism spectroscopy (FTIR-D). While SANS probes orientation on the length scale of the radius of gyration, ^{2}H-NMR, birefringence and FTIR-D monitor orientation on a segmental scale. The deformation of the elastomer chains appears to be affine on the different length scales.

Key words Orientation – deformation – thermoplastic elastomer

Introduction

The orientation behavior of polymers subjected to uniaxial strain has been investigated by a variety of methods [1–9]. Among the most important of these methods are infrared dichroism spectroscopy [1–4], small-angle neutron and x-ray scattering [5–7], birefringence [7], and deuteron nuclear magnetic resonance spectroscopy [2, 8, 9]. Here, we extend such studies to thermoplastic elastomers based on polybutadiene statistically modified by 4-(3,5-dioxo-1,2,4-triazoline-4-yl) isophthalic acid (U35A) via an ene-reaction. U35A can associate to larger clusters via hydrogen bonding [10]. Such systems behave similar to ionomers with the main difference being that the directed hydrogen bonds are accessible to characterization by a variety of methods. Differential scanning calorimetry shows besides the glass transition temperature of polybutadiene at approximately $-90\,^{\circ}C$ a glass transition at approximately $80\,^{\circ}C$ and endothermic transitions of the U35A domains at approximately $170\,^{\circ}C$, indicating a phase separation between U35A-side groups and polybutadiene [10].

In this paper the following questions will be addressed: i) What is the nature of the U35A-domains formed in a polybutadiene matrix and is there an influence of the hydrogen bonding side groups on the conformation of polybutadiene in the isotropic state?; ii) do the functional side groups orient upon uniaxial strain also?; and iii) do the elastomeric chains show an affine deformation upon uniaxial deformation? In order to answer these questions a combination of different methods will be used: small- and

Colloid & Polymer Science, Vol. 274, No. 8 (1996)

wide-angle x-ray scattering (SAXS, WAXS), small-angle neutron scattering (SANS), deuteron nuclear magnetic resonance spectroscopy (^{2}H-NMR), birefringence and infrared dichroism spectroscopy (FTIR-D).

Experimental

Preparation of the samples

Three different kinds of polybutadienes were used in this study. For ^{2}H-NMR experiments the polybutadiene chains contained deuterium in the 1- and 4-positions of the monomer, which was labeled by proton–deuteron exchange reaction on butadiene sulfone [11]. For the SANS and birefringence measurements blends of non-deuterated (h6) and perdeuterated polybutadienes (d6) were used, which were synthesized by Th. Wagner (Max-Planck Institut für Polymerforschung). A commercial cis-1,4-polybutadiene (CB10 from Hüls AG, Marl) had been used for the infrared dichroism experiments. The characteristics of the polymers are given in Table 1. The synthesis of 5-(3,5-dioxo-1,2,4-triazoline-4-yl)-isophthalic acid (U35A) is described elsewhere [10]. Polybutadienes were dissolved in dry tetrahydrofuran (THF) and reacted with solutions of U35A to give samples with 2 or 4 mol% (with respect to double bonds in the polymer) degree of modification (Fig. 1). After the completion of the ene-reaction (disappearance of the characteristic red color) the samples were reprecipitated from isopropanol, dissolved again in dry THF and cast into Petri dishes. Homogeneous films were obtained by slow evaporation of the solvent. In order to prepare samples for the SANS measurements deuterated and hydrogenated polymers (both modified and unmodified) were dissolved again and blend films were obtained by casting the mixed solutions into Petri dishes. To determine the structure factor of a single chain only one concentration of labeled chains is necessary in SANS experiments [12]. In both the modified and unmodified blends the amount of deuterated polymer was 30%.

Methods of investigation

All experiments reported here were performed at room temperature, if not indicated otherwise.

The SANS measurements to obtain the chain conformation of the isotropic samples were carried out on the SANS setup of Risø National Laboratory with a neutron wavelength $\lambda_{neutron}$ of 1 nm and a sample to detector distance of 6 m. Data were radially averaged. The SANS-measurements on the deformed samples were performed on the SANS-1 setup of GKSS, Geesthacht using $\lambda_{neutron}$ = 0.85 nm and a sample to detector distance of 9 m. The sample was fixed in a manually-driven stretching device. The scattering intensity was detected by a two-dimensional detector with a resolution of 64 * 64 data points. All SANS data were corrected for background scattering, incoherent scattering and transmission. Absolute scattering intensities were obtained by calibration with a water sample.

Table 1 Characterization of polybutadienes

Experiment	Sample	M_n (g/mol)	M_w/M_n (g/mol)
SANS, Birefringence	Poly-1,4-butadiene (d6)	80 000[a]	1.045[a]
	Poly-1,4-butadiene (h6)	80 000[a]	
^{2}H-NMR	Poly-1,4-butadiene (d3.5) 76% deuterated in the 1,4 positions[c]	70 000[b]	1.05[b]
SAXS, WAXS, FTIR-D	Poly cis-1,4-butadiene (h6) (CB10, Hüls AG)	200 000[b]	2[b]

[a] gel permeation chromatography calibrated to polybutadiene.
[b] gel permeation chromatorgraphy calibrated to polystyrene and subsequently corrected by a factor of 0.75 for polybutadiene.
[c] ^{1}H-NMR.

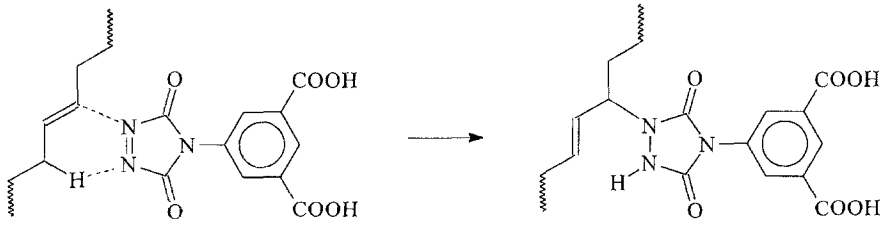

Fig. 1 Scheme of the ene-reaction of polybutadiene with U35A

The SAXS measurements were performed on a Kratky–Kompakt-Camera (A. Paar KG, Graz, Austria) using Cu-K_α-radiation with a wavelength of $\lambda_{x\text{-ray}} = 0.1542$ nm. The data were corrected for background scattering and normalized to the intensity at a distinct scattering vector.

The WAXS measurements were carried out on a Siemens Θ–Θ diffractometer using Cu-K_α radiation.

^{2}H-NMR spectra were recorded on a Bruker MSL-360 spectrometer operating at a frequency of 55.82 MHz. The spectra were obtained by a solid-echo pulse sequence followed by a Fourier transformation starting at the maximum of the echo as described elsewhere [13]. The length of the 90° pulse was always 2 μs. A description of the specially designed strain device is given in ref. [14].

Birefringence was measured by using a home-made setup equipped with a polarization modulation technique using a HeNe-laser operating at a wavelength of 633 nm. The laser passes subsequently through a linear polarizer, the sample, a quarter wave plate and finally a rotating polarizer to the detector [15].

Infrared dichroism was determined with a Bruker IFS88 spectrometer using a wire grid polarizer in conjunction with a photoelastic modulator at the Institut für Makromolekulare Chemie in Freiburg [16, 17].

Determination of orientation

Orientation of uniaxial materials can be described by an orientation distribution function $\rho(\alpha)$, expanded as:

$$\rho(\alpha) = \sum_{n=0}^{\infty} \left(n + \frac{1}{2}\right) \langle P_n(\cos\alpha)\rangle P_n(\cos\alpha) \,. \tag{1}$$

Here $P_n(\cos\alpha)$ is the Legendre polynomial of n-th order and brackets denote ensemble averages and α is the angle between a structural unit (segmental axis or a C-D-bond for example) and a reference direction (stretching direction). In the case of rotational isotropy around specified directions, e.g. C–D bonds on a cone around a segmental axis, the addition theorem of Legendre polynomials can be applied:

$$\langle P_2(\cos\alpha)\rangle = \langle P_2(\cos\theta)\rangle \cdot \langle P_2(\cos\gamma)\rangle \,. \tag{2}$$

Here, θ is the angle between the segmental axis and the stretching direction, γ is the angle between the segmental axis and respectively, the C-D bond (in case of ^{2}H-NMR), the long axis of the ellipsoid of the dielectric polarizability (in case of birefringence), or the direction of the transition moment of a particular vibration (in case of infrared dichroism). This relation is important since quite often the exact value of γ is not known. The angle α depends on the method used to measure orientation. For that reason the data sets obtained by different methods need to be normalized in order to compare them with each other.

The $\langle P_n(\cos\alpha)\rangle$ of the uniaxial orientation distribution function $\rho(\alpha)$ are obtained from the spatially averaged moments $\langle(\cos\alpha)^n\rangle$

$$\langle(\cos\alpha)^n\rangle = \frac{\sum_0^{\pi/2} I(\alpha)\cdot(\cos\alpha)^n \cdot \sin\alpha}{\sum_0^{\pi/2} I(\alpha)\cdot\sin\alpha} \tag{3}$$

and tabulated coefficients for Legendre polynomials [18]. $I(\alpha)$ is the intensity at the angle α with respect to the strain direction.

While Eq. (3) can be used directly in the case of scattering techniques like SANS, the evaluation of the averaged second order Legendre polynomial (which we will also call order parameter in the following) from ^{2}H-NMR requires a substitution of variables. Instead of a summation over angles a summation over frequencies is required. From the relation between orientation angle and frequency of the ^{2}H-NMR spectrum,

$$\Delta\nu = \pm\,\delta \cdot P_2(\cos\alpha)\cdot P_2(\cos\Omega) \,, \tag{4}$$

Eq. (3) can be rewritten as [19] (for $\Omega = 90°$)

$$\langle(\cos\alpha)^2\rangle = \frac{1}{3}\cdot\frac{\sum_{|\Delta\upsilon|}^{\delta} I(\Delta\nu)\cdot\left(\frac{\Delta\nu}{\delta}+1\right)^{\frac{1}{2}}}{\sum_{|\Delta\upsilon|}^{\delta} I(\Delta\nu)\cdot\left(\frac{\Delta\nu}{\delta}+1\right)^{-\frac{1}{2}}} \,, \tag{5}$$

where δ is the quadrupolar coupling constant (125 kHz for aliphatic C–D bonds [20]), $I(\Delta\nu)$ is the intensity of a pair of resonance lines with a splitting $\Delta\nu$ and Ω is the angle between magnetic field and stretching direction.

In elastomers well above the glass transition temperature the polymer chains are mobile. Then the frequency $\Delta\nu(\alpha)$ is averaged over the motion ($P_2(\cos\alpha)$ is Eq. (4) is then a time-averaged quantity) and a single quadrupole doublet results. In this case only the order parameter $\langle P_2(\cos\alpha)\rangle$ is reflected in the NMR spectrum, which now includes time and ensemble averages. In reality, the quadrupole splitting is often broadened and there has been a lot of discussion about the origin of the broadening of the spectra: in some cases dynamic heterogeneities were considered to be the reason for line broadening, i.e., different parts of the system relax on different time scales [21], in other studies the possibility of orientational distribution along network chains [22, 23] or different orientations of long and short network chains [24] were discussed. For the systems under study it was shown before that only approximately two monomer units in the neighborhood of the U35A-group behave solid like [25], but the corresponding contribution to the signal of the ^{2}H-NMR spectra does not lead to a significant broadening of the line shape, as was shown by an independent measurement of a

Colloid & Polymer Science, Vol. 274, No. 8 (1996)

stretched sample with the stretching direction oriented at the magic angle with respect to the magnetic field [14]. A rather narrow line shape was found which means that dynamical contributions to the broadening of the line shape are very small, since only the orientational contribution cancel according to Eq. (4). The correct separation of dynamical and orientational contributions to the line shape of the spectra would be deconvolution as outlined before [19]. However, the free induction decays measured under the magic angle (54.7°) must have a very high signal-to-noise ratio, because otherwise a large error is introduced within the deconvolution procedure. It was also shown by deuteron T_1 relaxation experiments on this system that dynamic contributions to the line shape are negligible [14]. Since there are almost no relaxations occurring in the system, which are comparable or ever slower than the ^{2}H-NMR time scale, this polymeric system is somewhere close to the liquid case. As described before [19], we subtract the order parameter in the unstrained state from the order parameter measured of the strained samples. This gives us the changes of $\langle P_2(\cos\alpha)\rangle$ from the unstrained state:

$$\Delta\langle P_2(\cos\alpha)_\lambda\rangle = \langle P_2(\cos\alpha)_\lambda\rangle_{\exp} - \langle P_2(\cos\alpha)_1\rangle_{\exp}\,, \qquad (6)$$

where λ is the strain ratio (=length/initial length) and brackets denote time and ensemble average. Note that $\Delta\langle P_2(\cos\alpha)\rangle$ becomes negative for the system under uniaxial strain, since the C–D bonds orient on average at angles larger than the magic angle with respect to the stretching direction.

Birefringence Δn of 1,4-polybutadiene is positive, since the polarizability along the chain axis is larger than perpendicular to it (the angle γ is around 0°, which means $\alpha \approx \theta$). Birefringence is proportional to the order parameter with the birefringence of a perfectly oriented polybutadiene Δn_0 being the proportionality constant:

$$\langle P_2(\cos\alpha)\rangle = \frac{\Delta n}{\Delta n_0}\,. \qquad (7)$$

Since we do not know Δn_0, we use Δn only as a qualitative indicator for $\langle P_2(\cos\alpha)\rangle$, which becomes positive upon uniaxial strain.

We use FTIR-D in this study only qualitatively to check for orientation of both the elastomer and the U35A side groups, so we refrain from a detailed description here.

Results and discussion

In Fig. 2 SAXS data of a polybutadiene modified with 2 mol% U35A at different temperatures show a maximum at approximately 0.6 nm^{-1}. The maximum decreases with increasing temperature and still exists at a temperature above the endothermic transition observed by differential scanning calorimetry. This is a clear indication of a microphase separation between elastomer and clusters of U35A units. A "correlation hole"-peak as observed in disordered block copolymers [26] cannot explain the maximum in these data, because the scattering contrast here originates from the electron density difference between U35A and polybutadiene. Since the U35A units are randomly distributed along the polymer backbone, no maximum can be expected in a scattering curve of a homogeneous melt. Similar SAXS data have been reported for another hydrogen bond assembly based on 4-(3,5-dioxo-1,2,4-triazoline-4-yl)-benzoic acid (U4A) randomly attached to a polybutadiene matrix [27]. Polyisobutylene containing one U4A unit at one chain end organizes into a two-dimensional (lamellar like) morphology as shown by transmission electron microscopy (TEM) and SAXS [28]. The first order maximum is the SAXS pattern corresponds in that case to the distance $d \approx 7$ nm between the lamellae observed by TEM. Thus, we assume the rather broad maxima in Fig. 2 to correspond to the average distance $d \approx 10$ nm between the clusters of U35A units. Since there is no indication of higher order maxima, the long-range order of these clusters should be low. WAXS data of a polybutadiene modified with 2 mol% U35A is compared with a low molecular weight model compound (U35A adduct of trans-butene) in Fig. 3. While the low molecular weight model compound shows discrete reflections indicating crystalline order, the polymer shows only an amorphous halo. Thus the polymeric backbone prevents the side groups from developing long-ranged crystalline order, although the material is microphase separated. However, some kind of structure must be present in the system because otherwise no melting should be observed. An

Fig. 2 SAXS traces of polybutadiene containing 2 mol% U35A at various temperatures: 20 °C (—), 100 °C (– – –), 200 °C (· · ·)

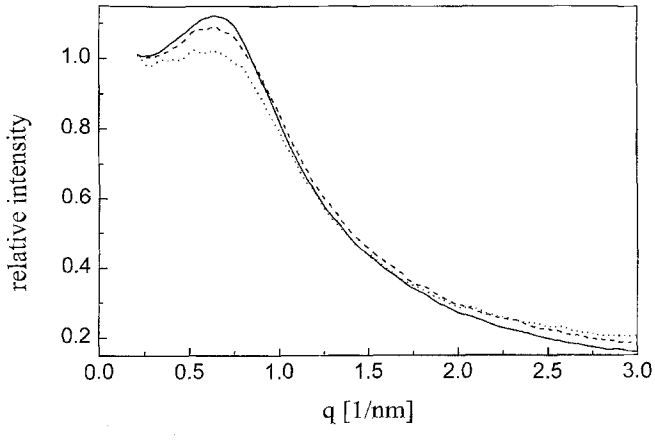

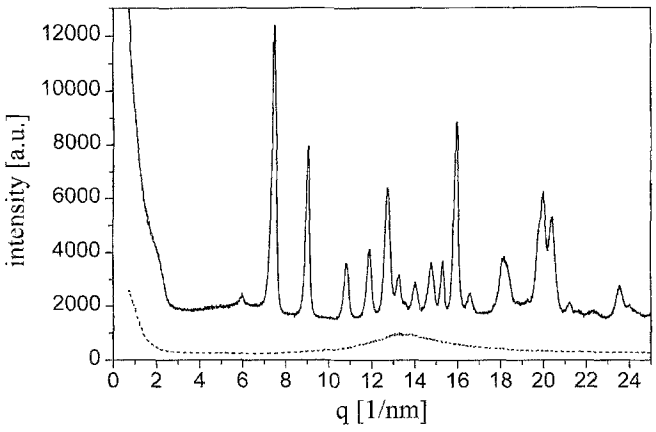

Fig. 3 WAXS traces of trans-butene-U35A (—) and polybutadiene containing 2 mol% U35A (– – –)

explanation could be the existence of non-crystalline spherulites as they have been observed for polyisobutylene-U4A [28]. While in that case the spherulites could be observed by polarized optical microscopy, the statistical modification of polybutadiene in our study prevents the system from formation of spherulites with a large enough size detectable by that technique. The energy of conversion associated with the endothermic peak in DSC could be related to a cooperative melting of hydrogen bonds within the amorphous clusters.

SANS traces from polybutadiene with and without U35A side groups in the unstrained state are almost identical. Thus the U35A microdomains do not change the chain conformation of polybutadiene significantly.

Before we discuss the deformation behavior of polybutadiene in these thermoplastic elastomers in more detail, first possible contributions of the U35A side groups to orientation, characterized by the strain ratio λ will be discussed. While the olefinic C–H stretching vibration shows dichroism upon strain (i.e., the absorptions of parallel and perpendicular polarized light differ from each other) (Fig. 4A), the carbonyl stretching vibration characteristic for U35A units shows no dichroism at all (Fig. 4B). Thus the U35A side groups do not orient macroscopically upon strain and will not contribute to intrinsic birefringence. Anisotropy of the U35A domains upon strain should lead to a form birefringence. Such a deformation of the U35A domains should be negligible for the small deformation ratios under study, because the melting temperature of U35A clusters is rather high. In Fig. 5 $\Delta\langle P_2(\cos\alpha)\rangle$ of ^{2}H-NMR is plotted versus birefringence. The linear relationship between the two data sets is a strong indication that only polybutadiene orients under strain, since ^{2}H-NMR monitors only polybutadiene. A possible form anisotropy of the solid U35A-domains

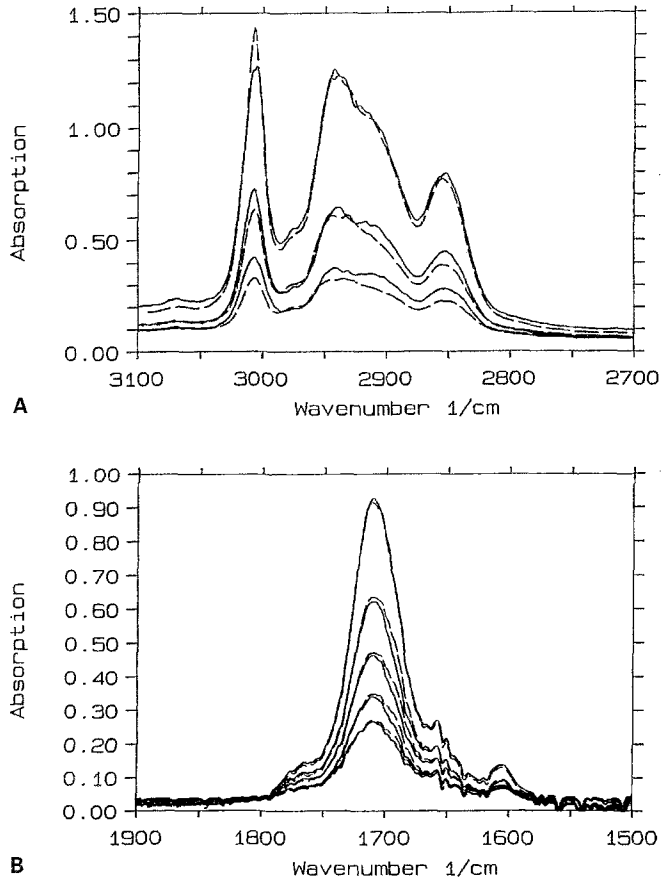

Fig. 4 FTIR-spectra of a polybutadiene containing 4 mol% U35A. **A** C–H stretching vibrations at $\lambda = 1, 3, 5$ (from top to bottom), **B** Carbonyl and aromatic ring stretching vibrations at $\lambda = 1, 2, 3, 4, 5$ (from top to bottom). Perpendicular (—) and parallel (– – –) polarization with respect to the strain direction

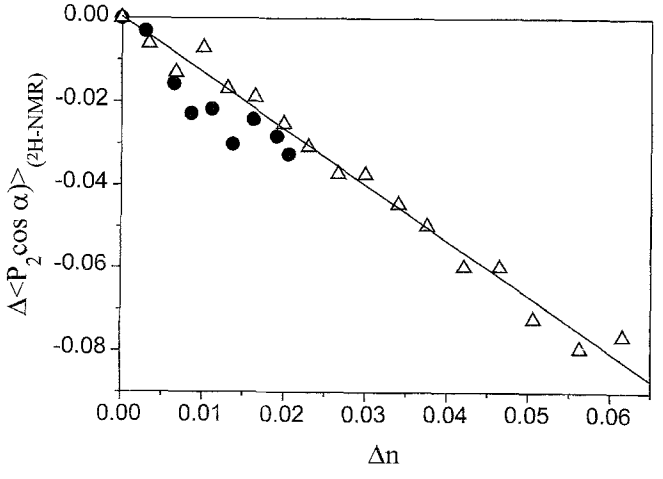

Fig. 5 Comparison of the order parameter obtained by ^{2}H-NMR with the birefringence Δn for polynbutadienes with (●) 2 mol% and (Δ) 4 mol% U35A

should obey a different dependence of strain thus leading to a more complex strain dependence of the birefringence. Since it is difficult to quantify the orientation from ^{2}H-NMR at the small strains under investigation with a high accuracy, birefringence will be considered as a more reliable measure for orientation on a segmental length scale in this study.

In order to determine orientation on the length scale of the chain size (radius of gyration), two-dimensional SANS was employed. Figure 6 shows as an example the two-dimensional SANS data for the sample with 2 mol% U35A at a strain ratio $\lambda = 1$ and $\lambda = 2$. A circular symmetry of the scattering pattern in the unstrained state becomes elliptically deformed by uniaxial strain, as it has been observed for PDMS-networks, too [29]. Straube et al. showed for polyisoprene networks a transition of the SANS patterns from elliptical to lozengic shape, which indicates a non-affine deformation behavior [30] and thus supports a theoretical treatment of rubber elasticity including the tube-model [31, 32]. For the small strains used in this study such a transition cannot be seen. Thus the question about affinity of the deformation behavior cannot be decided by SANS alone in this study.

As outlined in refs. [30, 33], the strain ratio on the length scale of the radius of gyration can be determined by subtracting the SANS pattern of the isotropic sample from the SANS pattern from the strained sample. This was done with the data from Fig. 6 and the result is shown in Fig. 7. The orientation angle α^* is related to the strain ratio of the chain [30, 33]:

$$\lambda = -\frac{1}{2} + \sqrt{\frac{1}{4} + \tan^2(\alpha^*)} \,. \tag{8}$$

Here, we obtain a strain ratio of $\lambda \approx 2.1 \pm 0.2$. This compares well with the macroscopic strain ratio and thus the deformation is affine on this length scale.

Performing an angular dependent Zimm analysis [34], the radius of gyration of a Gaussian chain can be determined for different angles with respect to the stretching direction:

$$\frac{\phi(1-\phi)k}{I(q_\alpha)} = \frac{1}{N} + a_\alpha^2 q_\alpha^2 \tag{9}$$

$$R_\alpha = \sqrt{\frac{N}{6}}\, a_\alpha \tag{10}$$

$I(q_\alpha)$ is the scattering intensity, k is the contrast factor, ϕ is the volume fraction of deuterated chains, N is the degree of polymerization, a_α is the length of a statistical segment in

Fig. 6 Two-dimensional SANS traces of polybutadiene modified with 2 mol% U35A. The lines connect points with equal scattering intensity. Values are decreasing with increasing distance from the beam-stop (rectangular area in the center) and are omitted for clarity. **A** $\lambda = 1$; **B** $\lambda = 2$

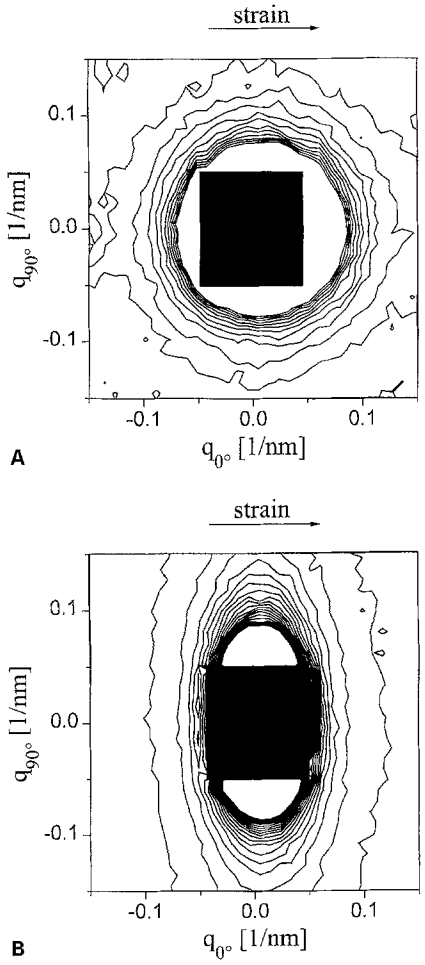

Fig. 7 Difference scattering pattern of Figs. 6a and b. Only the isointensity lines of both scattering patterns ($\Delta I = 0$) are shown. The straight lines are fits to determine the orientation angle α^*

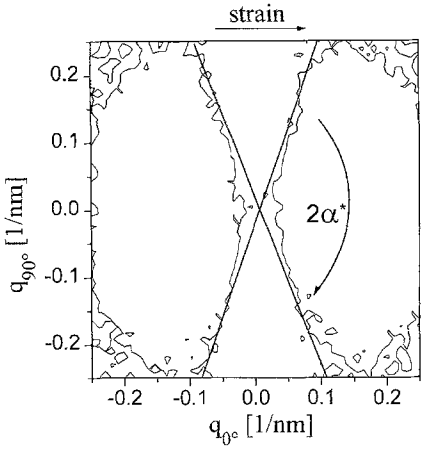

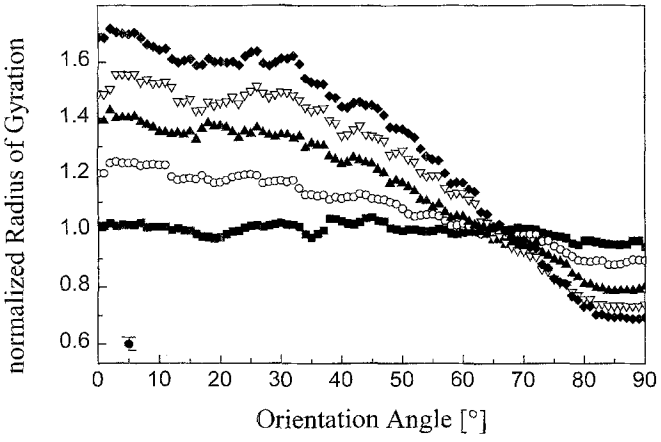

Fig. 8 Normalized radius of gyration radius of polybutadiene with 2 mol% U35A (with respect to the average value of the unstrained state) versus orientation angle for different strains (■) $\lambda = 1$, (○) $\lambda = 1.25$, (▲) $\lambda = 1.5$, (▽) $\lambda = 1.75$, (◆) $\lambda = 2$. The error in the data is indicated by the error bar (●)

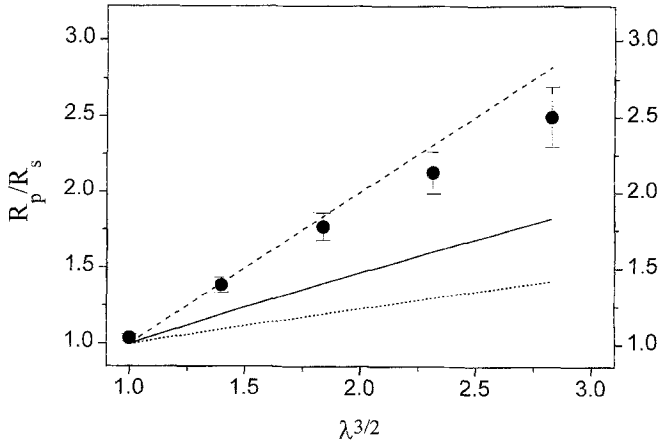

Fig. 9 Ratio of radius of gyration as a function of the strain function corresponding to affine deformation. (●) Polybutadiene with 2 mol% U35A; (···) James and Guth model (Phantom network); (—) Kuhn model (junction affine network); (– – –) affine network

angular direction α, q_α is the scattering vector in angular direction $\alpha (q = (4\pi/\lambda_{\text{neutron}}) \cdot \sin \Psi)$, ψ is half of the scattering angle. At scattering angle zero the scattering intensity is independent of the orientation angle (it contains only the molecular weight, (Eq. (9)). Figure 8 shows the radius of gyration normalized with respect to the unstrained state ($R_{\alpha,\lambda}/R_{\alpha,1}$) for different strain ratios as a function of orientation angle. The orientation angle α^* can be obtained in this plot from the intersection points where $R_{\alpha,\lambda}/R_{\alpha,1} = 1$. The ratio of the radii of gyration parallel (R_p) and perpendicular (R_s) to the stretching direction,

$$R_{p/s} = \frac{R_p}{R_s} \tag{11}$$

is useful for direct comparison with theoretical models. In Fig. 9 this ratio of the radii of gyration is shown as a function of the ratio between sample dimensions parallel and perpendicular to the stretching direction L_p/L_s. For the systems under study it was checked by measuring the change of thickness as a function of deformation that the sample volume does not change upon uniaxial deformation. So, we obtain:

$$\frac{L_p}{L_s} = \left[\frac{R_p}{R_s}\right]_{\text{affine}} = \frac{\lambda}{1/\sqrt{\lambda}} = \lambda^{3/2} . \tag{12}$$

In Fig. 9 the behavior according to the model of Kuhn [35, 36] for a junction-affine network [29, 37] is shown,

$$\left[\frac{R_p}{R_s}\right]_{\text{Kuhn}} = \sqrt{\frac{\lambda^3 + \lambda}{\lambda + 1}} \tag{13}$$

and it is obvious that the anisotropies observed experimentally are much larger than the theoretical prediction by Kuhn. Within experimental error an affine deformation behavior of the radius of gyration is observed for this system. The phantom model of James and Guth [38] would yield for an infinite large functionality of the network points (which are the U35A clusters) the same result as the Kuhn-model. For smaller functionalities the deviation from experiment becomes even larger, as is shown for a network with a functionality $f = 4$ [39], which would correspond to binary complexes of U35A.

$$\left[\frac{R_p}{R_s}\right]_{\text{James-Guth},f=4} = \sqrt{\frac{\lambda^3 + 3\lambda}{3\lambda + 1}} . \tag{14}$$

For chemically crosslinked polybutadiene networks and thermoplastic elastomers based on poly(styrene-*b*-butadiene-*b*-styrene) block copolymers [23, 24] and for polydimethylsiloxane networks experiments were much closer to the Kuhn-model or between the predictions of the Kuhn- and James and Guth-theory. This means that in those systems affinity may be achieved by the network junctions, but not for the whole system.

Analyzing the SANS data according to Eq. (3) for a given absolute vlaue of the scattering vector (or scattering angle) gives access to averaged Legendre polynomials of different order. The order parameters did not change within the scattering vector range covered by the experiment and were averaged to get a better signal-to-noise ratio. Besides Eq. (3), also the anisotropy of the radius of gyration can be used to obtain $\langle P_2(\cos\alpha)\rangle$. A relation known from dichroism spectroscopy relates the dichroic

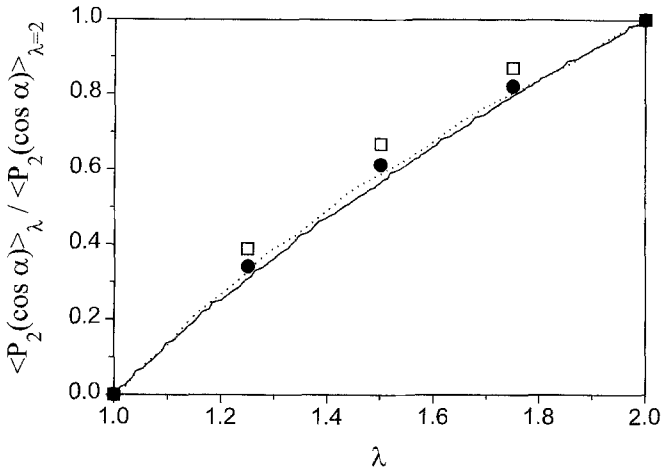

Fig. 10 Comparison of normalized order parameters as function of strain ratio from SANS using Eq. (3) (□) and Eq. (15) (●) and birefringence (—) for polybutatdiene with 2 mol% U35A and (····) for polybutadiene with 4 mol% U35A

ratio with $\langle P_2(\cos\alpha)\rangle$:

$$\langle P_2(\cos\alpha)\rangle \propto \frac{R_{p/s}-1}{R_{p/s}+2}. \tag{15}$$

To obtain information about the length scale dependence of orientation, the averaged second order Legendre polynomials need to be compared from different methods. As mentioned before, we cannot compare the averaged second order Legendre polynomials from SANS and birefringence directly with each other, since according to Eq. (2) the Legendre polynomial containing the angle γ must be introduced. To overcome this problem, the data sets are normalized to the values of the different Legendre polynomials at strain ratio $\lambda = 2$ (this value is chosen, because it is the maximum strain ratio at which measurements were performed with the different methods). In Fig. 10 the normalized data are shown. Within experimental error all normalized data sets show the same deformation dependence. Together with the conclusion of Figs. 7 and 9, this indicates that the orientation of the elastomer is affine also on the segmental length scale.

Conclusions

Polybutadiene modified with 4-(3,5-dioxo-1,2,4-triazoline-4-yl)-isophthalic acid (U35A) forms a microphase separated material containing *amorphous* U35A-clusters. This is probably due to the geometry of the hydrogen bonding complexes, which do not allow U35A to form an ordered cluster, when U35A is attached randomly to a polymer backbone. While in this case the polymeric nature of the backbone prevents the side group from forming an ordered domain, and no orientation of these domains upon strain is observed, the situation may become different when the geometry of the side group is changed. By using 4-(3,5-dioxo-1,2,4-triazoline-4-yl)-benzoic acid (U4A) instead of U35A it was shown that also the microphase separated U4A units orient upon uniaxial stretching [40].

The conformation of polybutadiene chains is not altered by the presence of these side groups in the unstrained state, at least no change of the radius of gyration is observed. This does not mean that the repeating units of the polymer, which are directly connected to the clusters are not influenced at all. However, the influence of the clusters on the chain conformation in the isotropic state is small due to the large flexibility of the elastomer chain. From comparison of the orientation measured by different methods it follows within experimental error that the deformation on short and long length scales is affine.

Acknowledgments V.A. thanks Th. Wagner and M. Stamm for the protonated and deuterated polybutadienes for SANS and M. Bach for the strain device for SANS measurements. V.A. further thanks W. Pyckhout-Hintzen for a helpful discussion. A.D. thanks C.D. Poon and D. Photinos for many helpful discussions. Financial support from the European Community (Large Installation Programme in Risø), the German Israeli Foundation GIF, the Deutsche Kautschukgesellschaft as well as a NATO travel grant are gratefully acknowledged.

References

1. Ward IM (1975) Structure and Properties of Oriented Polymers. Applied Science Publishers Ltd, London
2. Ward IM (1982) Developments in Oriented Polymers-1. Applied Science Publishers Ltd, London
3. Jasse B, Koenig JL (1979) J Macromol Sci-Rev Macromol Chem C17:61
4. Siesler HW (1984) Adv Polym Sci 65:1
5. Picot C (1982) Small Angle Neutron Scattering (SANS) by Amorphous Polymers. In: Pethrich RA, Richards RW (eds) Static and Dynamic Properties of the Polymeric Solid State. Reidel Publishing Company
6. Baltá-Calleja FJ, Vonk CG (1989) X-ray Scattering of Synthetic Polymers. In: Jenkins AD (ed) Polymer Science Library. Elsevier, Amsterdam
7. Stein RS, Norris FH (1965) J Polym Sci 21:381
8. Sotta P, Deloche B (1988) Polymer 29:1171
9. Schmidt-Rohr K, Spiess H-W (1994) Multidimensional Solid-State NMR and Polymers. Academic Press, Oxford
10. Hellmann J, Hilger C, Stadler R (1994) Polym Adv Technol 5:763
11. Cope AC, Berchthold GA, Ross DL (1961) J Am Chem Soc 83:3859

12. Gawrich W, Brereton MG, Fischer EW (1981) Polym Bull 4:687
13. Hentschel D, Spiess HW, Sillescu H (1984) Polymer 25:1078
14. Dardin A, Boeffel C, Spiess HW, Stadler R, Samulski ET (1995) In: Nakatani AI, Dadmun MD (eds) Flow Induced Structures in Polymers. ACS-Symposium Series 597:190–203
15. Fuller GG (1990) Annu Rev Fluid Mech 22:387
16. Abetz V, Fuller GG, Stadler R (1990) Polym Bull 23:447
17. Abetz V, Fuller GG, Stadler R (1991) Makromol Chem Macromol Symp 52:23
18. Abramowitz M, Stegun IA (1964) Handbook of Mathematical Functions. Dover Publications, New York
19. Jacobi MM, Abetz V, Stadler R, Gronski W Polymer, in press
20. Hentschel D, Spiess HW, Sillescu H, Voelkel R, Willenberg B (1976) Magn Reson Relat Phenom Proc Congr Ampere 19th, 381
21. Samulski ET (1985) Polymer 26:177
22. Gronski W, Stadler R, Jacobi MM (1984) Macromolecules 17:741
23. Poon CD, Samulski ET, Nakatani AI (1990) Makromol Chem Macromol Symp 40:109
24. Gronski W, Emeis D, Brüderlin A, Jacobi MM, Stadler R, Eisenbach CD (1985) British Polymer Journal 17:103
25. Dardin A, Stadler R, Boeffel C, Spiess HW (1993) Makromol Chem 194:3467
26. Leibler L (1980) Macromolecules 13: 1602
27. Hilger C, Stadler R (1992) Macromolecules 25:6670
28. Schirle M, Hoffmann I, Pieper T, Kilian HG, Stadler R (1996) Polym Bull 36:95
29. Beltzung M, Picot C, Herz J (1984) Macromolecules 17:663
30. Straube E, Urban V, Pyckhout-Hintzen W, Richter D, Glinka CJ (1995) Phys Rev Lett 74:4464
31. Heinrich G, Straube E (1983) Acta Polym 34:589
32. Heinrich G, Straube E (1987) Polym Bull 17:247
33. Boué F (1987) Adv Polym Sci 82:47
34. Zimm BH (1948) J Chem Phys 16:1093
35. Kuhn W (1936) Kolloid-Z 76:258
36. Treloar LRG (1975) The Physics of Rubber Elasticity, 3rd ed. Clarondon Press, Oxford
37. Benoît H, Duplessix R, Ober R, Cotton JP, Farnoux B, Jannink G (1975) Macromolecules 8:451
38. James HM, Guth E (1949) J Polym Sci 4:153
39. Pearson DS (1977) Macromolecules 10:696
40. Abetz V, Hilger C, Stadler R (1991) Makromol Chem Macromol Symp 52:131